

Solving the Reactive Power Dispatch Optimization for Large Scale System

M. Nungky Ibrahim^{1*}, Tri Wrahatnolo², Rifqi Firmansyah³
^{1,2,3}electrical departement, State University of Surabaya.
^{1,2,3}A5 Building Ketintang Campus, Surabaya 60231, Indonesia
¹nungkyibrahim@gmail.com

Abstract— Reactive power dispatch (RPD) is a crucial optimization task in power system operation because it seeks the optimal settings of control variables, such as generator voltages, transformer tap positions, and shunt VAR compensators, to reduce active power loss while satisfying operating constraints [file:1]. This study investigates the application of the fmincon solver and particle swarm optimization (PSO) to the RPD problem on three benchmark IEEE test systems, namely the 30-bus, 57-bus, and 118-bus networks [file:1]. For the IEEE 30-bus system, the minimum active power loss obtained by fmincon and PSO was 4.5480 MW and 4.4858 MW, respectively, corresponding to loss reductions of 21.88% and 22.95% from the initial value of 5.8223 MW [file:1]. For the IEEE 57-bus system, the power loss was reduced from 0.2846 p.u. to 0.2473 p.u. by fmincon and to 0.2362 p.u. by PSO, equivalent to reductions of 13.11% and 17.01%, respectively [file:1]. These results show that both methods are effective for large-scale RPD optimization, while PSO generally provides the best performance among the compared techniques in terms of active power loss minimization. The contribution of this study lies in providing a focused comparison between a deterministic nonlinear programming solver and a population-based metaheuristic approach across different system sizes, thereby demonstrating their practical suitability for large-scale reactive power optimization

Keywords: reactive power dispatch, fmincon solver, PSO power loss reduction.

I. INTRODUCTION

In an electricity generation system, the target of reactive power dispatch (RPD) is selecting the best value of the control variable (CV) that optimizes the stated objective function like power losses minimization, voltage profile enhancement, and fuel cost minimization whilst complying with the constraints from the unit and system [1]. The target can be reached through the appropriate setting of reactive power (RP) variables such as switchable VAR source, setting of transformer tap, and voltage magnitude of generator [2], [3].

In the past, the RPD problem for enhancing power system security and economy has become more attentive. The goal of optimal RPD is to reduce active power (AP) losses as well as to enhance the profile of the voltage. Thus, the RPD problem should be optimized either for active power losses (APL) reduction or voltage profile improvement (VPI) [4], [5].

In the literature, the traditional optimization algorithm to overcome the problem of RPD have been carried out such as mixed integer programming [6], lambda iteration method [7], dynamic programming [8], newton method [9], gradient-based method [10] and branch-bound method [11]. These algorithms have a drawback in controlling the problems with discontinuous landscape or the nonconvex as well as discrete variables. In other hand, several modern meta-heuristic approaches have been proposed such as particle swarm optimization (PSO) [12], tabu search (TS) [13], ant colony optimization [14], genetic algorithms (GA) [15], artificial neural networks (ANN) [16], simulated

annealing (SA) [17], differential evolution (DE) [18], bacterial foraging algorithm [19], and artificial bee colony (ABC) [20].

In this paper, the fmincon solver and PSO provided by MATLAB code are introduced to find the solution to the RPD problem. These techniques are employed to reduce AP losses. The techniques have been tested on IEEE 30-, 57- and 118-buses test systems in addition to assessing the capability of the techniques. Furthermore, the outcomes are compared with other previously studied optimization techniques via comparative analysis.

The rest of this work is structured as follows. A problem formulation will be explained in Section II. Section III fmincon solver. In section IV, simulation result and analysis is discussed. Conclusions are presented at the end of the study in Section V.

II. METHODS

In this study, the reactive power dispatch (RPD) problem is formulated as an optimization problem aimed at minimizing active power (AP) losses, total voltage deviation (TVD), and fuel cost, while satisfying all unit and system constraints. The control variables (CVs) include generator voltage magnitudes, transformer tap settings, and shunt VAR compensator outputs. The optimization was implemented using MATLAB 2017a, running on an AMD A9-9425 RADEON R5, 3.10 GHz processor with 12.0 GB RAM. Two optimization techniques were employed: the fmincon solver and Particle Swarm Optimization (PSO).

The objective functions used in this study are defined as follows. The real power loss minimization is formulated as:

$$f_1 = P_{loss} = \sum_{k=1}^{n_l} g_k [V_i^2 + V_j^2 - 2V_i V_j \cos(\delta_i - \delta_j)] \quad (1)$$

where n_l defines the number of transmission lines, g_k denotes the k -th line conductance, V_i and V_j are the voltage magnitudes at buses i and j of the k -th line, and δ_i, δ_j are the corresponding voltage phase angles. The voltage profile improvement (VPI) objective is calculated as:

$$f_2 = \sum_{i \in NL} |V_i - 1.0| \quad (2)$$

where NL is the number of load buses. The equality constraints represent the load flow equations:

$$P_{Gi} - P_{Di} - V_i \sum_{j=1}^{NB} V_j [G_{ij} \cos(\delta_i - \delta_j) + B_{ij} \sin(\delta_i - \delta_j)] = 0 \quad (3)$$

$$Q_{Gi} - Q_{Di} - V_i \sum_{j=1}^{NB} V_j [G_{ij} \sin(\delta_i - \delta_j) - B_{ij} \cos(\delta_i - \delta_j)] = 0 \quad (4)$$

where NB denotes the buses number, P_G defines the generation of active, Q_G defines the generation of RP, P_D defines the load AP, Q_D defines the load RP, G_{ij} and B_{ij} denote the transfer conductance as well as susceptance between bus i and bus j . The inequality constraints limit the generator voltages, reactive power outputs, transformer tap settings, and shunt VAR compensations as follows:

$$V_{Gi}^{min} \leq V_{Gi} \leq V_{Gi}^{max}, i = 1, \dots, NG \quad (5)$$

$$Q_{Gi}^{min} \leq Q_{Gi} \leq Q_{Gi}^{max}, i = 1, \dots, NG \quad (6)$$

$$T_i^{min} \leq T_i \leq T_i^{max}, i = 1, \dots, NT \quad (7)$$

$$Q_{ci}^{min} \leq Q_{ci} \leq Q_{ci}^{max}, i = 1, \dots, NC \quad (8)$$

This paper covers the differential evolution (DE), Salp swarm algorithm (SSA), and chaotic bat algorithm (CBA) optimization techniques modified JAYA algorithm (MJAYA), sine-cosine algorithm (SCA), which are briefly described in this section.

The SCA generates numerous initial irregular candidate solutions and requires them to change outwards or approach the optimum solution using a sine-cosine mathematical representation. Also, many irregular and adaptive variables are incorporated with this algorithm to bring to the fore investigation and take advantage of the search space in different breakthroughs of optimization. SCA algorithm pseudo-code is given in Fig. 1 below [21].

Here, X_i^t represent the location of the present result in i th size at t -th iteration, $r_1/r_2/r_4$ are the irregular numbers, P_i^t refers to the location of the endpoint in i th size, r_4 denotes an irregular number in $[0,1]$, and $\|$ denotes the absolute value.

$$X_i^{t+1} = \begin{cases} X_i^t + r_1 \times \sin(r_2) \times |r_3 P_i^t - X_i^t|, & r_4 < 0.5 \\ X_i^t + r_1 \times \cos(r_2) \times |r_3 P_i^t - X_i^t|, & r_4 \geq 0.5 \end{cases}$$

As the above equations show, there are four main parameters in SCA: $r_1, r_2, r_3,$ and r_4 .

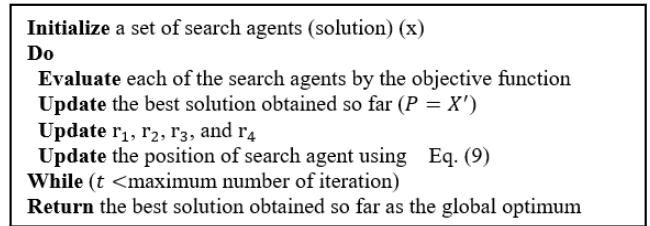


Figure 1 General procedures of the SCA Algorithm.

Fig. 1 reveals that the SCA begins the procedure of optimization by a group of irregular results and afterward stores the optimal results acquired until now, allocates it as the endpoint, and revises other results concerning it. It stops the optimization procedure when the repetition counter proceeds more than the peak number of repetitions by default.

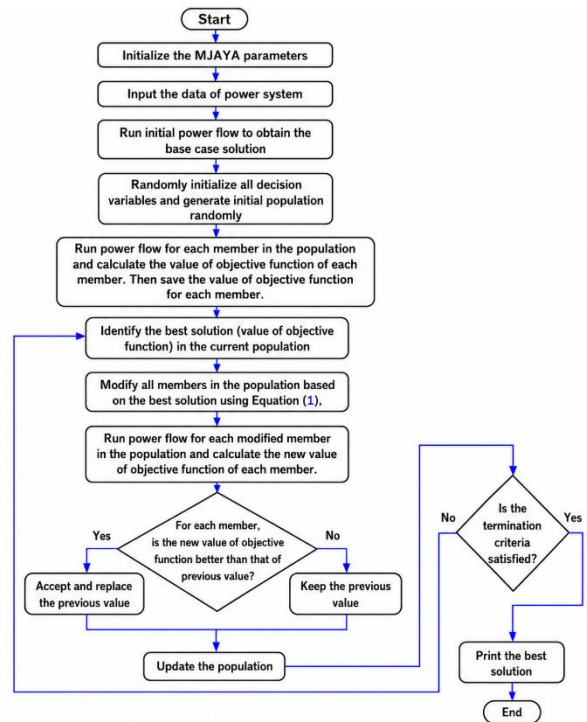


Figure 2 Flowchart of MJAYA for solving optimal power flow problem.

The MJAYA was proposed in [22] to solve the disadvantage of the main JAYA algorithm. The MJAYA can be acquired by varying the expression used to upgrade the results on the basis of the optimal and bad solutions. JAYA is a populace-based algorithm introduced in 2016 [23]. As an advantage, it does not require any adjusting procedure for the variables to obtain the global result of the optimization issue. In the suggested algorithm, the component with the optimal fitness value of the objective function is utilized just to upgrade the values of the other components, implying that the elite component in the populace behaves as a lead to remaining components in the populace to improve their locations to an area close to the optimal-known location. The flow diagram of MJAYA is illustrated in fig 2.

$$X'_{j,d,k} = X_{j,d,k} + r_{1,j,k} \times (X_{j,worst,k} - |X_{j,d,k}|) - L \times r_{2,j,k} \times (|X_{j,d,k}|^2 - X_{j,best,k}^2) \quad (10)$$

The main inspiration of the SSA is the swarming nature of salp when steering and searching in the ocean. The utmost objective of a one-objective optimizer is to find the global optimal. In the SSA, the disciple salps move behind the foremost salp. SSA pseudo-code is presented in Fig 3 below.

$$x_j^1 = \begin{cases} F_j + c_1((ub_j - lb_j)c_2 + lb_j), & c_3 \geq 0 \\ F_j - c_1((ub_j - lb_j)c_2 + lb_j), & c_3 < 0 \end{cases} \quad (11)$$

Here, x_j^1 shows the location of the foremost salp in the j th size, F_j is the location of the sustenance origin in the j th size, ub_j indicates the top bound of j th size, lb_j indicates the bottom bound of j th size, c_1 , c_2 , and c_3 are irregular numbers.

c_1 is the most important variable in SSA owing to taking advantage and investigation balancing and is defined as:

$$c_1 = 2e^{-\left(\frac{4l}{L}\right)^2} \quad (12)$$

where l is the current iteration and L is the maximum number of iterations.

$$x_j^i = \frac{1}{2}(x_j^i + x_j^{i-1}) \quad (13)$$

Here, $i \geq 2$ and x_j^i reveals the location of i th disciple salp in j th size. With Equ. (11) and (13), the salp chains are modeled.

```

Initialize the salp population  $x_i$  ( $i = 1, 2, \dots, n$ ) considering  $ub$  and  $lb$ 
while (end condition is not satisfied)
    Calculate the fitness of each search agent (salp)
     $F$  = the best search agent
    Update  $c_1$  by Eq. (12)
    for each salp ( $x_i$ )
        if ( $i == 1$ )
            Update the position of the leading salp by Eq. (11)
        else
            Update the position of the follower salp by Eq. (13)
        end
    end
    Amend the salps based on the upper and lower bounds of variables
end
return  $F$ 
    
```

Figure 3. SSA algorithm Pseudocode.

The SSA begins rounding the global optimal by starting many salps with irregular locations as shown in Fig 3 [24]. afterward determines the fitness of individual salp, determines the salp (optimal fitness), and allocates the location of the optimal salp to the parameter F as the origin sustenance the salp chain pursued. Meanwhile, c_1 is upgraded using Eq. (12). For each size, the location of the foremost salp is upgraded with Eq. (11) and the location of foremost salps is upgraded by Eq. (13). If any of the salps move out of the search space, it will be taken back to the borders. All the procedures above excluding the initialization are repetitively carried out till the satisfaction of a termination benchmark.

The BA as a new metaheuristic was introduced by Yang, while chaos was introduced into BA by [25] to raise its worldwide search movement, which gives rise to chaos-based BA was proposed for robust global optimization. As regards this algorithm, various chaotic configurations were utilized to put back the variables in BA. Also, chaotic maps were used in four various strategies to change the BA various as well as enhance the behavior, which gives rise to a group of BAs or various deviants of the chaotic BA. CBA flow diagram is given in fig 4

The Fmincon solver is the solver to determine the least restrained non-linear multiple parameter functions. The syntax of fmincon is available in ref [26].

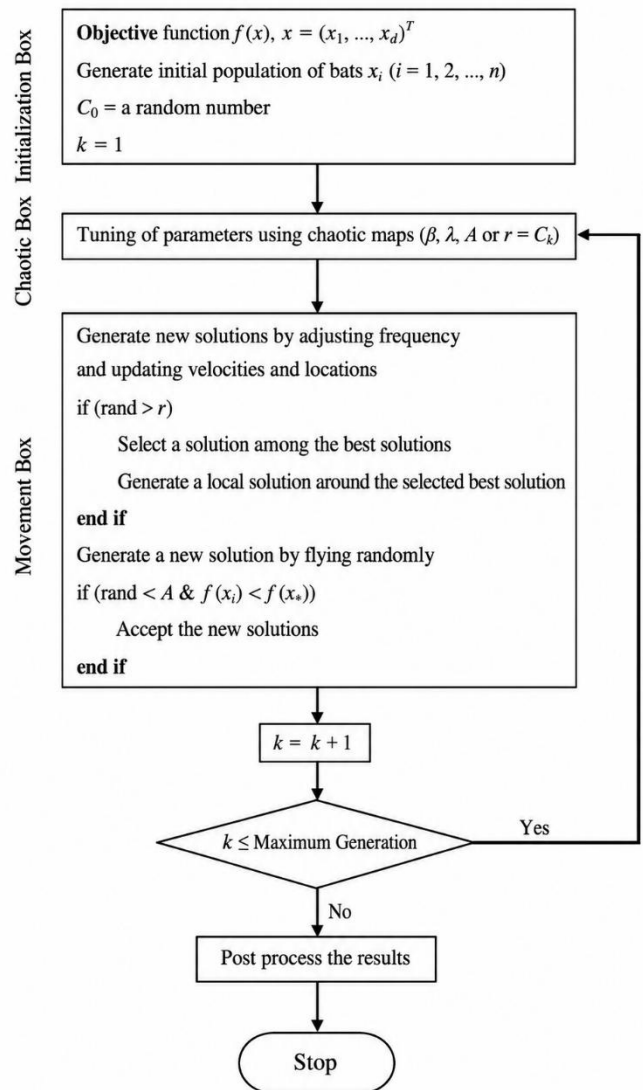


Figure 4 Flowchart of a CBA schematic.

For extensive optimization problems, the Fmincon utilizes the credence domain step. Individual repetition of the algorithm infers rounding up the results of a big linear expressions configuration by utilizing the conjugate slope technique with the prerequisite. Fmincon utilizes user-specified Hessian (H) for the target function. It rounds up the Hessian utilizing determinate differences, while fmincon utilizes a Sequential

QP method for moderate size optimization problems. In this approach, a QP sub-problem is worked out at individual repetition. An approximate H of the Lagrangian is upgraded at individual repetition and a line search is conducted utilizing a quality function. The QP sub-question is worked out utilizing an active group method [27].

The techniques were validated on three standard IEEE test systems: the 30-bus, 57-bus, and 118-bus systems. These systems represent small-to-large scale power networks and are widely used as benchmark cases in the literature [28], [29]. For the IEEE 30-bus system, voltage magnitude limits are set between 0.95–1.1 p.u. for generator buses and 0.95–1.05 p.u. for load buses, with transformer tap settings in the range of 0.9–1.1 p.u. and shunt VAR compensations between 0–0.05 p.u. For the IEEE 57-bus system, the search space includes 25 dimensions covering 7 generator voltages, 15 transformer taps, and 3 reactive power sources. For the IEEE 118-bus system, 131 control variables are considered, with voltage boundaries of 0.94–1.06 p.u., transformer tap boundaries of 0.90–1.10 p.u., and shunt VAR boundaries of 0–0.3 p.u.

III. RESULT AND DISCUSSION

This section presents the simulation results of the fmincon solver and PSO technique applied to the RPD problem across three IEEE test systems. The results are organized by test system and objective function, followed by comparative analysis against previously reported methods.

A. IEEE 30-Bus System

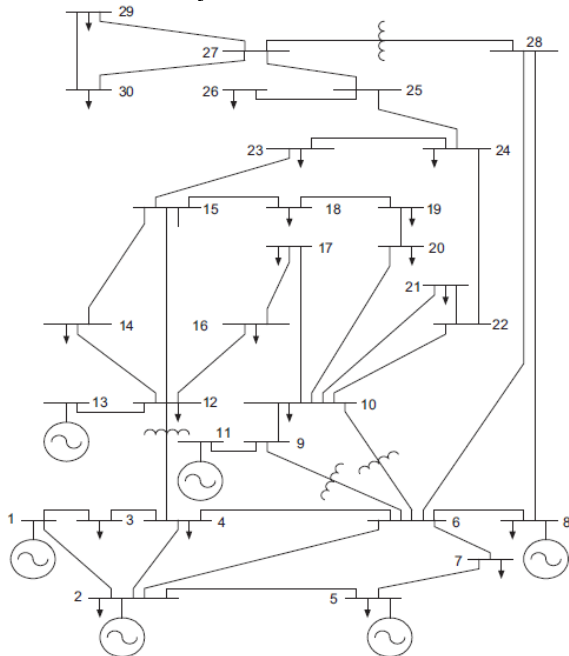


Figure 5 IEEE 30-bus test system

The system as illustrated in Fig. 5 consist of 6 gen-units (GU) (1, 2, 5, 8, 11 links) and 13, 41 transmission cables (TL), 4 adjusting tap-varying transformers (TCT). Moreover, 24 demand links in the company of 2.834 p.u. and 1.262 p.u. for the two AP and RP loads. The system information of the gen price coefficients, the links, cables, and the restrictions of <https://doi.org/10.26740/inajeee.v9n1>

the control and state parameters are reported by [28], [29]. The restriction on voltage magnitude is taking into account from 0.95 to 1.1 p.u. for the whole gen links. These restrictions are placed from 0.95 to 1.05 p.u. for the remaining links. The solution of nine SVARCs changes between 0 and 0.05 p.u. while the tap settings are resolved to vary within the domain 0.9 and 1.1 p.u.

1) Scenario 1: AP loss minimization for IEEE 30-Bus System

In the first scenario, the fmincon solver and PSO technique provided by MATLAB are executed with a reduction of AP losses as the target function for the considered bus system. The solvers achieve a minimum loss of 4.5480 MW and 4.4858 MW for fmincon and PSO respectively. The optimum values of the CV are provided in Table 1 for fmincon and PSO respectively. To show the effectiveness of the fmincon solver and PSO in terms of previously studied approaches in the area of optimizing optimal RPD to minimize AP loss, the optimized solutions are compared with the solutions of DE [2], SCA [30], MJAYA [22], SSA [31] as well as the CBA [32]. The outcomes of AP loss for different techniques are illustrated in Table 1. The fmincon AP loss is greatly minimized by about 21.88% in comparison with the starting value. For the PSO, it is minimized by around 22.95. But, the percentage minimization in AP loss when compared to the starting value is 21.76% at DE, 17.31% at SCA, 20.58% at MJAYA 20.72% at SSA, as well as 12.26% at CBA as shown in Fig.6. It is observed that fmincon and PSO give better results than other previously reported results with various techniques.

Table 1. Optimal settings of control variables of active power loss minimization for different Technique on IEEE 30-bus system

Control variable	Initial	Fmincon	PSO	DE [2]
V_1	1.0500	1.0999	1.1000	1.1000
V_2	1.0400	1.0943	1.0922	1.0931
V_5	1.0100	1.0748	1.0707	1.0736
V_8	1.0100	1.0868	1.1000	1.0756
V_{11}	1.0500	1.0999	1.1000	1.1000
V_{13}	1.0500	1.0999	1.1000	1.1000
T_{11}	1.0780	1.0189	0.9036	1.0650
T_{12}	1.0690	0.9000	0.9169	0.9097
T_{15}	1.0320	0.9834	0.9065	0.9867
T_{36}	1.0680	0.9669	0.9101	0.9689
Qc_{10}	0.0000	4.9957	5.0000	5.0000
Qc_{12}	0.0000	4.9957	4.9999	5.0000
Qc_{15}	0.0000	4.9893	4.9998	5.0000
Qc_{17}	0.0000	4.9973	5.0000	5.0000
Qc_{20}	0.0000	4.9829	5.0000	4.406
Qc_{21}	0.0000	4.9985	5.0000	5.0000
Qc_{23}	0.0000	3.7225	4.8357	2.8004
Qc_{24}	0.0000	4.9984	4.9998	5.0000

Qc_{29}	0.0000	2.1769	2.4060	2.5979
Power Losses (MW)	5.8223	4.5480	4.4858	4.5550

Table 2. Optimal settings of control variables of active power loss minimization for different Technique on IEEE 30-bus system (2)

Control variable	SCA [30]	MJAYA [22]	SSA [31]	CBA [32]
V_1	1.1000	1.1000	1.1000	1.045
V_2	1.0907	1.0919	1.0937	1.0376
V_5	1.0879	1.0670	1.0745	1.0138
V_8	1.0742	1.0698	1.0760	1.0158
V_{11}	1.1000	1.0953	1.1000	1.0764
V_{13}	1.1000	1.0684	1.0980	1.0374
T_{11}	1.1000	0.9838	1.0234	0.9927
T_{12}	1.0588	1.0350	0.9064	0.9754
T_{15}	0.9000	1.0029	0.9779	0.9825
T_{36}	1.1000	1.0009	0.9725	0.9625
Qc_{10}	0.0000	4.9111	0.3382	4.9074
Qc_{12}	0.3220	5.0000	4.3628	3.0239
Qc_{15}	4.5128	5.0000	4.9891	3.3911
Qc_{17}	0.0000	5.0000	4.4849	4.8860
Qc_{20}	3.0436	4.3801	4.4474	4.2147
Qc_{21}	1.8970	5.0000	5.0000	4.6343
Qc_{23}	0.5739	4.0931	3.3318	4.6343
Qc_{24}	4.1247	5.0000	4.9772	3.1860
Qc_{29}	3.5914	4.7324	2.4617	2.1936
Power Losses (MW)	4.8139	4.6235	4.6156	5.1081

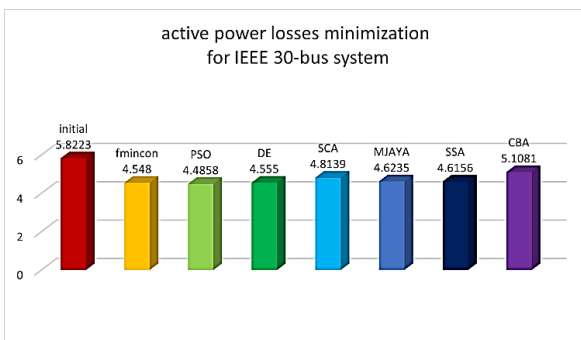


Figure 6. active power losses of IEEE 30-bus test system

2) Scenario 2: voltage deviation minimization for IEEE 30-Bus System

In the second scenario, the fmincon solver and PSO technique provided by MATLAB are run with total voltage deviation minimization as the objective function for IEEE 30-Bus System. The optimal values of the control variables are given

in the second and third columns of Table 2 for fmincon and PSO respectively. To show the effectiveness of the fmincon solver and PSO in terms of previously studied approaches in the area of optimizing optimal RPD to minimize total voltage deviation, the optimized solutions are compared with the solutions of DE [2], OGSA [3], and GSA [3]. The total voltage deviation of fmincon is greatly minimized by about 0.1502. For the PSO, it is minimized by around 0.0873. However, the total voltage deviation of OGSA is 0.0640, 0.0676 at GSA and 0.0911 at DE as shown in Fig. 7.

Table 3. Optimal settings of control variables of total voltage deviation minimization for different Technique on IEEE 30-bus system

Control Variable	Fmincon	PSO	OGS A [3]	GSA [3]	DE [2]
V_1	1.0162	1.0007	0.9746	0.9838	1.010
V_2	1.0195	0.9901	1.0273	1.0448	0.9918
V_5	1.0281	1.0331	0.9965	1.0203	1.0179
V_8	1.0348	1.0424	0.9982	0.9991	1.0183
V_{11}	1.0370	1.0799	0.9826	1.0770	1.0114
V_{13}	1.0268	1.0136	1.0403	1.0439	1.0282
T_{11}	0.9627	1.0457	0.9909	0.9000	1.0265
T_{12}	0.9578	0.9000	1.0629	1.1000	0.9038
T_{15}	0.9836	0.9905	1.0762	1.0505	1.0114
T_{36}	0.9612	0.9692	1.0117	0.9619	0.9635
Qc_{10}	2.6462	4.9242	0.0246	0.0000	4.9420
Qc_{12}	2.5396	3.5205	0.0175	0.4735	1.0885
Qc_{15}	2.6128	5.0000	0.0283	5.000	4.9985
Qc_{17}	2.6387	0.0001	0.0403	0.000	0.2393
Qc_{20}	2.7242	5.0000	0.000	5.000	4.9958
Qc_{21}	2.6858	5.0000	0.0270	0.000	4.9075
Qc_{23}	2.6940	5.0000	0.0385	4.9998	4.9863
Qc_{24}	2.7352	5.0000	0.0257	5.000	4.9663

Qc_{29}	2.7275	2.5866	0.000	5.000	2.2325
TVD (p.u)	0.1502	0.0873	0.0640	0.0676	0.0911

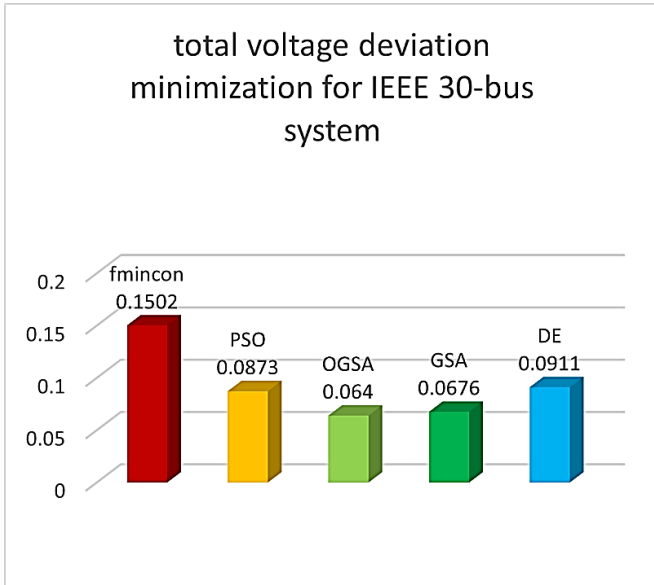


Figure 7. total voltage deviation minimization of IEEE 30-bus test system

3) Scenario 3: fuel cost minimization for IEEE 30-Bus System

In the scenario 3, the fmincon solver and PSO technique provided by MATLAB are run with fuel cost minimization as the objective function for IEEE 30-Bus System. The optimal values of the control variables are given in the second and third columns of Table 3 for fmincon and PSO respectively. To show the effectiveness of the fmincon solver and PSO in terms of previously studied approaches in the area of optimizing optimal RPD to minimize fuel cost, the optimized solutions are compared with the solutions of DE [2], and TLBO [33]. The fuel cost minimization of fmincon is greatly minimized by about 798.38. For the PSO, it is minimized by around 798.381. However, fuel cost minimization of TLBO presented in Fig. 8 is 799.071, and 799.2891 at DE.

Table 4. Optimal settings of control variables fuel cost minimization for different Technique on IEEE 30-bus system

Control Variable	Fmincon	PSO	TLBO [33]	DE [2]
P_1	176.2600	176.260	177.057	176.2592
P_2	48.7000	48.7000	48.6973	48.5602
P_5	21.6700	21.6700	21.3044	21.3402
P_8	21.2711	21.2711	21.0811	22.0553
P_{11}	11.7600	11.7600	11.8843	11.7785
P_{13}	12.1020	12.1020	12.0000	12.0217
V_1	1.0250	0.9648	1.1000	1.0999

V_2	1.0250	0.9670	1.0878	1.0890
V_5	1.0250	0.9871	1.0617	1.0659
V_8	1.0250	1.0671	1.0694	1.0697
V_{11}	1.0250	1.1000	1.1000	1.0965
V_{13}	1.0250	1.0004	1.1000	1.0996
T_{11}	1.0008	0.9577	1.0447	1.0429
T_{12}	1.0005	0.9383	0.9000	0.9179
T_{15}	0.9999	1.1000	0.9863	1.0190
T_{36}	1.0004	0.9762	0.9657	0.9896
Qc_{10}	1.6692	5.0000	0.0000	4.5453
Qc_{12}	1.6692	3.0255	0.0000	4.4158
Qc_{15}	1.6692	0.6731	0.0000	4.1734
Qc_{17}	1.6692	0.0000	0.0000	2.5171
Qc_{20}	1.6692	3.6345	0.0000	2.0916
Qc_{21}	1.6692	2.0470	0.0000	4.1990
Qc_{23}	1.6692	4.8943	0.0000	2.5527
Qc_{24}	1.6692	1.8110	0.0000	4.3812
Qc_{29}	1.6692	0.8253	0.0000	2.7503
Fuel Cost (\$/h)	798.38	798.381	799.071	799.2891

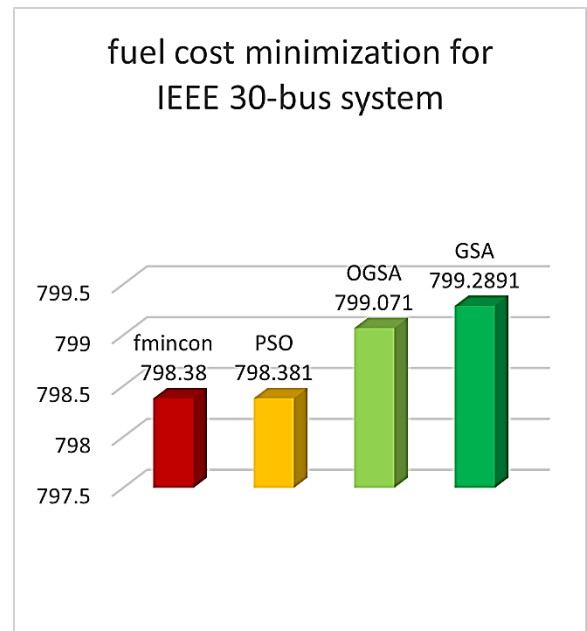


Figure 8. total fuel cost minimization of IEEE 30-bus test system

B. IEEE 57-Bus System

The bus system as depicted in Fig. 9 comprises eighty TLs, seven GUs (at the links 1, 2, 3, 6, 8, 9, 12), and fifteen branches under demand TCT branches are utilized as a test system 2. These RP sources are taken into account at links 18, 25, and 53. Line details, bus information, parameter limits, and the starting values of the CVs are obtained.

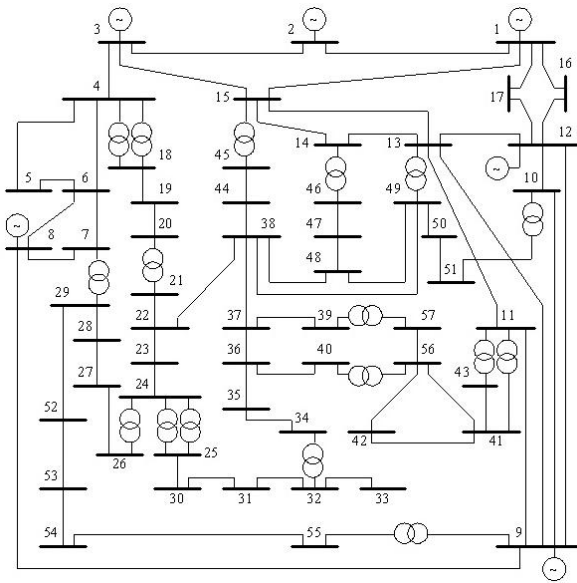


Figure 9. IEEE 57-bus test system

The scenario configuration search space has twenty-five sizes, including seven gen-voltages, fifteen TTs, and three RP sources. The system demands are expressed as: $P_L = 12.508 p.u.$, $Q_L = 3.364 p.u.$ The initial gross productions and Plosses are: $P_G = 12.79 p.u.$, $Q_G = 3.45 p.u.$, $P_{Loss} = 0.28 p.u.$, $Q_{Loss} = 1.24 p.u.$ There are five bus voltages in per unit. outside the restrictions: $V_{25} = 0.938$, $V_{30} = 0.92$, $V_{31} = 0.9$, $V_{32} = 0.926$, $V_{33} = 0.924$.

1) Scenario 4: AP Loss minimization for IEEE 57-Bus System

To evaluate the scalability of the fmincon solver and PSO and to display its capability to deal with extensive systems, the IEEE 57-bus system is used. In the scenario 4, the fmincon solver and PSO technique provided by MATLAB are executed with a reduction of AP losses as the target function for the chosen bus system. The solvers achieve a minimum loss of $0.2473 p.u.$ and $0.2362 p.u.$ for fmincon and PSO respectively. The best values of the CVs are presented in Table 4 for fmincon and PSO respectively. To show the efficacy of the fmincon solver and PSO in terms of previously studied approaches in the area of optimizing optimal RPD to minimize AP loss, the best outcomes are compared with solutions obtained using the following techniques: Nonlinear programming (NLP), Canonical Genetic algorithm (CGA), adaptive GA (AGA), Local DE (L-DE) and L-SACP-DE and their AP loss values are presented in Table 2. The Fmincon and PSO AP losses are greatly minimized by about 13.11% and 17.01% in comparison with the starting values. But, the percentage minimization in AP loss as shown in Fig. 9 when compared to the starting value is 8.99% at NLP, 11.31% at CGA 13.57% at AGA, 2.28% at L-DE, and 1.93% at L-SACP-DE. Observation of the results reveals that both Fmincon and PSO give better results than other previously reported results with various techniques.

Table 5. Optimal settings of control variables of active power loss minimization for different Technique on IEEE 57-bus system

Control Variable	Initial	Fmincon	PSO	NLP [35]
V_1	1.04	1.0474	1.0600	1.06
V_2	1.01	1.0600	1.0512	1.06
V_3	0.985	1.0021	1.0567	1.053
V_6	0.95	1.0259	1.0600	1.06
V_8	1.005	1.0333	1.0600	1.06
V_9	0.98	1.0600	0.9904	1.06
V_{12}	1.015	1.0146	1.0399	1.06
T_{4-18}	0.97	0.9000	0.9000	0.91
T_{4-18}	0.978	0.9000	0.9000	1.06
T_{21-20}	1.043	0.9886	0.9893	0.93
T_{24-26}	1.043	0.9885	0.9867	1.08
T_{7-29}	0.967	0.9000	0.9000	1.00
T_{34-32}	0.975	0.9789	0.9804	1.09
T_{11-41}	0.955	0.9000	0.9000	0.92
T_{15-45}	0.955	0.9000	0.9000	0.91
T_{14-46}	0.9	0.9000	0.9000	0.98
T_{10-51}	0.93	0.9086	0.9117	0.98
T_{13-46}	0.895	0.9000	0.9000	0.98
T_{11-43}	0.958	0.9000	0.9000	0.98
T_{40-46}	0.958	1.0200	1.0141	0.98
T_{39-57}	0.98	0.9869	0.9833	1.08
T_{9-55}	0.94	0.9000	0.9000	1.03
QC_{18}	0	9.9997	9.9993	0.083
QC_{25}	0	5.9000	5.9000	0.0086
QC_{23}	0	6.3000	6.3000	0.011
Power Losses (pu)	0.2846	0.2473	0.2362	0.2590

Table 6. Optimal settings of control variables of active power loss minimization for different Technique on IEEE 57-bus system (2)

Control Variable	CGA [35]	AGA [35]	L-DE [35]	L-SACP-DE [35]
V_1	0.968	1.027	1.039	0.988
V_2	1.049	1.011	1.046	1.054
V_3	1.0567	1.033	1.051	1.027
V_6	0.987	1.001	1.023	0.967
V_8	1.0223	1.051	1.053	1.0552
V_9	0.991	1.051	0.945	1.024
V_{12}	1.004	1.057	0.990	1.009

T_{4-18}	0.92	1.03	1.02	1.05
T_{4-18}	0.92	1.02	0.91	1.05
T_{21-20}	0.97	1.06	0.97	0.95
T_{24-26}	0.90	0.99	0.91	0.98
T_{7-29}	0.91	1.10	0.96	0.97
T_{34-32}	1.10	0.98	0.99	1.09
T_{11-41}	0.94	1.01	0.98	0.92
T_{15-45}	0.95	1.08	0.96	0.91
T_{14-46}	1.03	0.94	1.05	1.08
T_{10-51}	1.09	0.95	1.07	0.99
T_{13-46}	0.90	1.05	0.99	0.91
T_{11-43}	0.90	0.95	1.06	0.94
T_{40-46}	1.00	1.01	0.99	0.99
T_{39-57}	0.96	0.94	0.97	0.96
T_{9-55}	1.00	1.00	1.07	1.10
Q_{c18}	0.084	0.0168	0	0
Q_{c25}	0.0081	0.0153	0	0
Q_{c23}	0.0537	0.0388	0	0
Power Losses (pu)	0.2524	0.2456	0.2781	0.2791

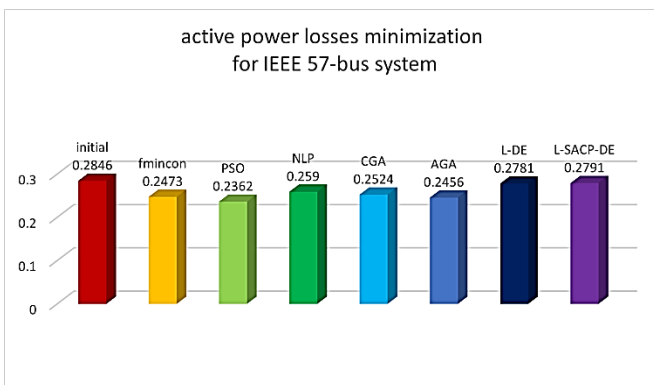


Figure 10. active power losses minimization of IEEE 57-bus test system

2) Scenario 5: total voltage deviation minimization for IEEE 57-Bus System

In the scenario 5, the fmincon solver and PSO technique provided by MATLAB are run with total voltage deviation minimization as the objective function for IEEE 57-Bus System. The optimal values of the control variables are given in the second and third columns of Table 5 for fmincon and PSO respectively. To show the effectiveness of the fmincon solver and PSO in terms of previously studied approaches in the area of optimizing optimal RPD to minimize total voltage deviation, the optimized solutions are compared with the solutions of OGSA [3]. The total voltage deviation of fmincon is greatly minimized by about 0.7995. For the PSO, it is minimized by around 0.6725. However, the total voltage deviation of OGSA is 0.6982 as shown in Fig. 10.

Table 7. Optimal settings of control variables of total voltage deviation minimization for different Technique on IEEE 57-bus system

Control Variable	Fmincon	PSO	OGSA [3]
V_1	1.0227	1.0100	1.0138
V_2	0.9998	1.0229	0.9608
V_3	1.0260	1.0365	1.0173
V_6	1.0034	1.0344	0.9898
V_8	1.0249	1.0297	1.0362
V_9	1.0397	0.9837	1.0241
V_{12}	1.0265	1.0503	1.0136
T_{4-18}	0.9894	1.0888	0.9833
T_{4-18}	0.9885	0.9080	0.9503
T_{21-20}	0.9808	0.9728	0.9523
T_{24-26}	1.0564	1.0640	1.0036
T_{7-29}	0.9506	0.9525	0.9778
T_{34-32}	0.9257	0.9065	0.9146
T_{11-41}	0.9457	0.9000	0.9454
T_{15-45}	0.9354	0.9154	0.9265
T_{14-46}	0.9432	0.9854	0.9960
T_{10-51}	0.9667	1.0082	1.0386
T_{13-46}	0.9457	0.9000	0.9060
T_{11-43}	0.9614	0.9604	0.9234
T_{40-46}	1.0153	1.0041	0.9871
T_{39-57}	0.9885	0.9001	1.0132
T_{9-55}	0.9859	0.9918	0.9372
Q_{c18}	8.7511	0.5024	0.0463
Q_{c25}	4.8103	5.8999	0.0590
Q_{c23}	5.0933	6.2999	0.0628
TVD (p.u)	0.7995	0.6725	0.6982

total voltage deviation minimization for IEEE 57-bus system

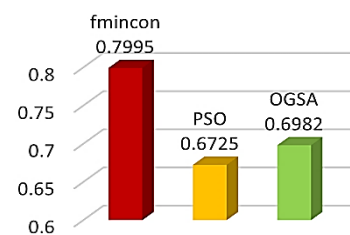


Figure 11. total voltage deviation minimization of IEEE 57-bus test system

3) Scenario 6: fuel cost minimization for IEEE 57-Bus System

The IEEE 57-bus system includes 7 generator units at buses

In the scenario 6, the fmincon solver and PSO technique provided by MATLAB are run with fuel cost minimization as the objective function for IEEE 57-Bus System. The optimal values of the control variables are given in the second and third columns of Table 6 for fmincon and PSO respectively. To show the effectiveness of the fmincon solver and PSO in terms of previously studied approaches in the area of optimizing optimal RPD to minimize fuel cost, the optimized solutions are compared with the solutions of IMFO [34]. The fuel cost minimization of fmincon is greatly minimized by about 41,620.85. For the PSO, it is minimized by around 41620.847. However, fuel cost minimization of IMFO presented in Fig. 11 is 41,667.15.

Table 8. Optimal settings of control variables of fuel cost minimization for different Technique on IEEE 57-bus system

Control Variable	Fmincon	PSO	IMFO [34]
PG_1	143.5900	143.5900	143.601
PG_2	86.5720	86.5720	86.593
PG_3	45.5100	45.5100	45.508
PG_6	74.6500	74.6500	74.668
PG_8	461.0070	461.0070	461.009
PG_9	91.9900	91.9900	92.001
PG_{12}	361.2520	361.2520	362.260
V_1	1.0015	0.9742	1.0513
V_2	1.0011	0.9400	1.0524
V_3	0.9985	0.9400	1.0396
V_6	0.9982	0.9400	1.037
V_8	1.0006	1.0392	1.0548
V_9	0.9982	0.9400	1.0375
V_{12}	1.0015	0.9879	1.0314
T_{4-18}	0.9967	1.0082	1.0104
T_{4-18}	0.9974	1.0451	0.9786
T_{21-20}	1.0039	0.9364	1.034
T_{24-26}	1.0039	0.9796	1.0175
T_{7-29}	0.9965	1.0028	0.9764
T_{34-32}	0.9971	0.9005	0.9581
T_{11-41}	0.9960	0.9906	0.9000
T_{15-45}	0.9960	1.1000	0.9622
T_{14-46}	0.9987	1.0454	0.9552
T_{10-51}	0.9966	0.9525	0.9627
T_{13-46}	0.9987	0.9270	0.9243
T_{11-43}	0.9961	0.9046	0.9615
T_{40-46}	0.9961	1.1000	0.9855
T_{39-57}	0.9976	0.9248	0.9550
T_{9-55}	0.9961	1.1000	0.9805
QC_{18}	8.9056	4.5782	9.4129
QC_{25}	4.8171	5.9000	12.971
QC_{23}	5.2152	1.3783	13.409

Fuel Cost (\$/h)	41,620.85	41,620.84	41,667.15
------------------	-----------	-----------	-----------

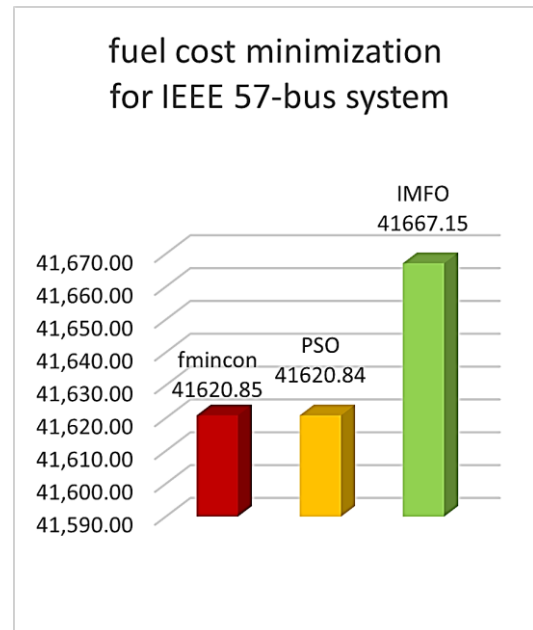


Figure 12. total fuel cost minimization of IEEE 57-bus test system

C. IEEE 118-Bus System

To evaluate the efficiency of fmincon and PSO, the IEEE 118-bus system is used for a large power test system. That large power test system consists of transmission lines: 186, generators power: 54 units, tap-changer transformers: 9 and shunt VAR compensators: 14. Moreover, 64 load buses with 42.42 p.u. for real power and 14.38 p.u. for reactive power. The real AP loss in initial condition is 1.3286 p.u. Moreover, this system comprises the control variable: 131. The boundaries of the voltage are 0.94 p.u. and 1.06 p.u. The boundaries of the transformer tap are 0.90 p.u. and 1.10 p.u. The shunt VAR available boundaries is 0–0.3 p.u.

1) Scenario 7: Active Power Loss minimization for IEEE 118-Bus System

To evaluate the scalability of the fmincon solver and PSO and to display its capability to deal with extensive systems, the IEEE 118-bus system is used. In the scenario 7, the fmincon solver provided by MATLAB are executed with a reduction of AP losses as the target function for the chosen bus system. The solvers achieve a minimum loss of 119.794 for fmincon. The best values of the CVs are presented in Table 7 for fmincon and PSO respectively. To show the efficacy of the fmincon solver and PSO in terms of previously studied approaches in the area of optimizing optimal RPD to minimize AP loss, the best outcomes are compared with solutions obtained using the following techniques: GSA and OGSA and their AP loss values are presented in Table 7. The Fmincon and PSO AP losses are greatly minimized by about 119.794 and 114.58 in comparison with the starting values. However, the minimization in AP loss as shown in Fig. 12 is 126.99 at OGSA and 127.76 at GSA . Observation of the results reveals that both Fmincon and PSO give better results than other previously reported results with various techniques.

Table 9. Optimal settings of control variables of power loss minimization for different Technique on IEEE 118-bus system

Control Variable	Fmincon	PSO	OGSA	GSA
V ₁	1.0446	0.9535	1.0350	0.9600
V ₄	1.0217	1.0377	1.0554	0.9620
V ₆	1.0408	1.0290	1.0301	0.9729
V ₈	1.0473	1.0600	1.0175	1.0570
V ₁₀	1.0521	1.0164	1.0250	1.0885
V ₁₂	0.9876	1.0454	1.0410	0.9630
V ₁₅	1.0436	1.0600	0.9973	1.0127
V ₁₈	0.9684	1.0463	1.0047	1.0069
V ₁₉	1.0511	1.0221	0.9899	1.0003
V ₂₄	1.0222	1.0600	1.0287	1.0105
V ₂₅	1.0482	1.0600	1.0600	1.0102
V ₂₆	1.0513	1.0600	1.0855	1.0401
V ₂₇	1.0117	1.0524	1.0081	0.9809
V ₃₁	1.0033	1.0406	0.9948	0.9500
V ₃₂	1.0459	1.0178	0.9993	0.9552
V ₃₄	0.9979	1.0600	0.9958	0.9910
V ₃₆	1.0319	1.0584	0.9835	1.0091
V ₄₀	1.0068	1.0308	0.9981	0.9505
V ₄₂	1.0079	1.0340	1.0068	0.9500
V ₄₆	1.0197	1.0465	1.0355	0.9814
V ₄₉	1.0352	1.0600	1.0333	1.0444
V ₅₄	0.9720	1.0314	0.9911	1.0379
V ₅₅	1.0305	0.9800	0.9914	0.9907
V ₅₆	1.0509	1.0600	0.9920	1.0333
V ₅₉	1.0275	1.0574	0.9909	1.0099
V ₆₁	1.0349	1.0600	1.0747	1.0925
V ₆₂	1.0241	1.0280	1.0753	1.0393
V ₆₅	1.0536	1.0600	0.9814	0.9998
V ₆₆	1.0487	1.0600	1.0487	1.0355
V ₆₉	1.0437	1.0600	1.0490	1.1000
V ₇₀	0.9829	1.0579	1.0395	1.0992
V ₇₂	1.0116	1.0414	0.9900	1.0014
V ₇₃	1.0097	1.0288	1.0547	1.0111
V ₇₄	1.0447	1.0600	1.0167	1.0476
V ₇₆	1.0386	0.9498	0.9972	1.0211
V ₇₇	1.0521	1.0600	1.0071	1.0187
V ₈₀	1.0247	1.0455	1.0066	1.0462
V ₈₅	1.0543	1.0075	0.9893	1.0491
V ₈₇	1.0085	1.0457	0.9693	1.0426

Table 10. Optimal settings of control variables of power loss minimization for different Technique on IEEE 118-bus system

Control Variable	Fmincon	PSO	OGSA	GSA
V ₈₉	1.0470	1.0600	1.0527	1.0955
V ₉₀	1.0215	1.0417	1.0290	1.0417
V ₉₁	1.0211	1.0447	1.0297	1.0032
V ₉₂	1.0560	1.0206	1.0353	1.0927
V ₉₉	1.0165	1.0406	1.0395	1.0433
V ₁₀₀	1.0259	1.0455	1.0275	1.0786
V ₁₀₃	0.9830	1.0600	1.0158	1.0266
V ₁₀₄	1.0209	0.9770	1.0165	0.9808
V ₁₀₅	1.0449	1.0412	1.0197	1.0163
V ₁₀₇	0.9847	1.0010	1.0408	0.9987
V ₁₁₀	1.0405	0.9797	1.0288	1.0218
V ₁₁₁	0.9967	1.0178	1.0194	0.9852
V ₁₁₂	0.9742	0.9936	1.0132	0.9500
V ₁₁₃	1.0159	1.0468	1.0386	0.9764
V ₁₁₆	1.0057	1.0600	0.9724	1.0372
T ₈	1.0172	1.0121	0.9568	1.0659
T ₃₂	1.0205	0.9684	1.0409	0.9534
T ₃₆	1.0127	1.0079	0.9963	0.9328
T ₅₁	1.0085	1.0124	0.9775	1.0884
T ₉₃	1.0070	1.0284	0.9560	1.0579
T ₉₅	1.0221	1.0532	0.9956	0.9493
T ₁₀₂	0.9935	1.0343	0.9882	0.9975
T ₁₀₇	0.9744	0.9994	0.9251	0.9887
T ₁₂₇	1.0183	1.0499	1.0661	0.9801
Qc ₅	-0.1639	-0.309	-0.331	0.00
Qc ₃₄	2.0950	0.0034	0.0480	7.46
Qc ₃₇	-0.1511	-0.299	-0.249	0.00
Qc ₄₄	1.9688	0.1286	0.0328	6.07
Qc ₄₅	2.3718	9.4013	0.0383	3.33
Qc ₄₆	2.4117	8.8992	0.0545	6.51
Qc ₄₈	2.2409	0.2041	0.0181	4.47
Qc ₇₄	2.1288	8.4451	0.0509	9.72
Qc ₇₉	2.2854	14.557	0.1104	14.25
Qc ₈₂	2.5299	19.420	0.0965	17.49
Qc ₈₃	2.2951	9.5939	0.0263	4.28
Qc ₁₀₅	2.2446	11.998	0.0442	12.04
Qc ₁₀₇	1.8854	0.0001	0.0085	2.26
Qc ₁₁₀	1.9475	5.4594	0.0144	2.94
Power Losses (pu)	119.794	114.58	126.99	127.76

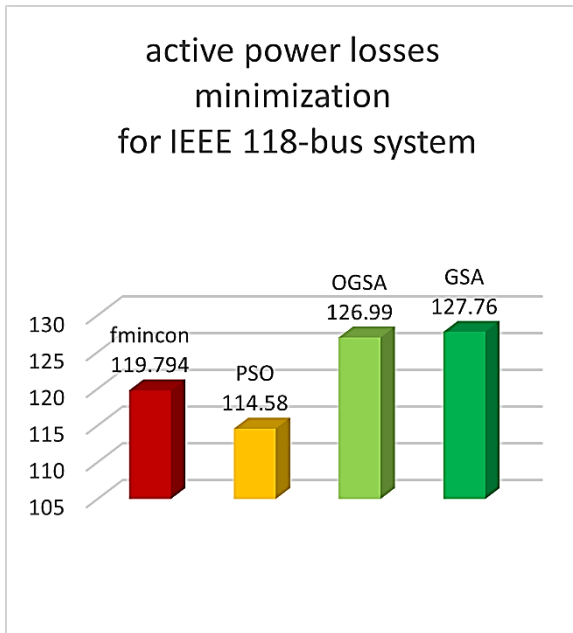


Figure 13. active power losses minimization of IEEE 118-bus test system

2) Scenario 8: Total voltage deviation minimization for IEEE 118-Bus System

In the scenario 8, the fmincon solver and PSO technique provided by MATLAB are run with total voltage deviation minimization as the objective function for IEEE 118-Bus System. The optimal values of the control variables are given in the second of Table 8 for fmincon. To show the effectiveness of the fmincon solver in terms of previously studied approaches in the area of optimizing optimal RPD to minimize total voltage deviation, the optimized solutions are compared with the solutions of OGSA [3]. The total voltage deviation of fmincon is greatly minimized by about 0.7995. For the PSO, it is minimized by around 0.5684. However, the total voltage deviation of OGSA is 0.3666.

Table 11. Optimal settings of control variables of total voltage deviation minimization for different Technique on IEEE 118-bus system

Control Variable	Fmincon	OGSA
V ₁	1.0167	1.0388
V ₄	1.0019	0.9872
V ₆	0.9884	0.9925
V ₈	0.9894	0.9905
V ₁₀	0.9945	0.9919
V ₁₂	1.0332	1.0077
V ₁₅	1.0088	1.0034
V ₁₈	0.9981	0.9773
V ₁₉	1.0256	1.0324
V ₂₄	1.0050	1.0285
V ₂₅	1.0029	0.9705
V ₂₆	0.9979	1.0175
V ₂₇	1.0089	1.0117

V ₃₁	1.0027	1.0014
V ₃₂	1.0115	0.9988
V ₃₄	1.0099	1.0158
V ₃₆	0.9908	0.9916
V ₄₀	1.0082	1.0132
V ₄₂	1.0022	0.9892
V ₄₆	1.0122	1.0607
V ₄₉	1.0040	1.0031
V ₅₄	1.0210	1.0236
V ₅₅	1.0000	1.0176
V ₅₆	1.0053	1.0149
V ₅₉	0.9998	1.0584
V ₆₁	1.0021	0.9829
V ₆₂	1.0098	1.0562
V ₆₅	0.9884	0.9724
V ₆₆	1.0094	1.0020
V ₆₉	0.9994	0.9827
V ₇₀	1.0126	0.9997
V ₇₂	1.0019	1.0123
V ₇₃	1.0073	0.9960
V ₇₄	1.0123	1.0232
V ₇₆	1.0132	1.0015
V ₇₇	1.0355	1.0124
V ₈₀	1.0196	1.0226
V ₈₅	1.0360	1.0117
V ₈₇	1.0069	1.0058

Table 12. Optimal settings of control variables of total voltage deviation minimization for different Technique on IEEE 118-bus system

Control Variable	Fmincon	OGSA
V ₈₉	1.0108	1.0076
V ₉₀	1.0000	0.9753
V ₉₁	1.0000	0.9836
V ₉₂	1.0315	1.0272
V ₉₉	1.0000	0.9612
V ₁₀₀	1.0237	1.0032
V ₁₀₃	1.0000	0.9843
V ₁₀₄	1.0000	0.9880
V ₁₀₅	1.0257	1.0003
V ₁₀₇	1.0036	1.0033
V ₁₁₀	1.0166	1.0040
V ₁₁₁	1.0000	1.0331
V ₁₁₂	1.0000	0.9877
V ₁₁₃	0.9967	0.9705
V ₁₁₆	0.9810	1.0270
T ₈	1.0032	0.9841

T_{32}	1.0001	1.0377
T_{36}	0.9930	0.9573
T_{51}	0.9838	0.9952
T_{93}	0.9977	0.9622
T_{95}	0.9878	1.0320
T_{102}	1.0000	1.0137
T_{107}	0.9930	0.9795
T_{127}	0.9765	0.9985
Qc_5	-0.2002	-0.2403
Qc_{34}	5.1942	0.0371
Qc_{37}	-0.1500	-0.0437
Qc_{44}	4.9782	0.0375
Qc_{45}	5.1252	0.0400
Qc_{46}	5.0746	0.0749
Qc_{48}	5.1828	0.0796
Qc_{74}	4.9718	0.0883
Qc_{79}	5.3668	0.1218
Qc_{82}	5.6058	0.0380
Qc_{83}	5.0471	0.0627
Qc_{105}	5.1828	0.0830
Qc_{107}	3.9302	0.0459
Qc_{110}	3.9302	0.0221
TVD (p.u)	0.5684	0.3666

P_{24}	0.0125	0.0125
P_{25}	193.6700	193.670
P_{26}	279.7220	279.722
P_{27}	15.8441	15.8441
P_{31}	7.2543	7.2543
P_{32}	13.4763	13.4763
P_{34}	2.5040	2.5040
P_{36}	8.8714	8.8714
P_{40}	49.9442	49.9442
P_{42}	42.0478	42.0478
P_{46}	19.1282	19.1282
P_{49}	193.6080	193.608
P_{54}	50.1543	50.1543
P_{55}	31.6590	31.6590
P_{56}	34.7532	34.7532
P_{59}	149.6010	149.601
P_{61}	147.8370	147.837
P_{62}	0.0022	0.0022
P_{65}	353.2840	353.284
P_{66}	349.1850	349.185
P_{69}	454.9120	454.912
P_{70}	0.9058	0.9058
P_{72}	0.0237	0.0237
P_{73}	0.2558	0.2558
P_{74}	16.2229	16.2229
P_{76}	22.2712	22.2712
P_{77}	0.0002	0.0002
P_{80}	429.6960	429.696
P_{85}	0.0255	0.0255
P_{87}	3.6354	3.6354
P_{89}	504.4180	504.418
P_{90}	0.0021	0.0021
P_{91}	0.0000	0.0000
P_{92}	0.0003	0.0003
P_{99}	0.0112	0.0112
P_{100}	231.1060	231.106
P_{103}	38.0594	38.0594
P_{104}	0.0174	0.0174
P_{105}	4.5931	4.5931
P_{107}	30.4984	30.4984
P_{110}	0.4828	0.4828
P_{111}	35.4211	35.4211
P_{112}	39.8141	39.8141
P_{113}	0.0152	0.0152
P_{116}	0.0036	0.0036
V_1	0.9940	1.0106
V_4	0.9940	1.0269

3) Scenario 9: fuel cost minimization for IEEE 118-Bus System

In the scenario 9, the fmincon solver provided by MATLAB are run with fuel cost minimization as the objective function for IEEE 118-Bus System. The optimal values of the control variables are given in the second of Table 9 for fmincon. To show the effectiveness of the fmincon solver in terms of previously studied approaches in the area of optimizing optimal RPD to minimize fuel cost, the optimized solutions are compared with the solutions of TLBO [33]. The fuel cost minimization of fmincon is greatly minimized by about 129,682.647. However, fuel cost minimization of TLBO is 129,682.844.

Table 13. Optimal settings of control variables of fuel cost minimization for different Technique on IEEE 118-bus system

Control Variable	Fmincon	TLBO
P_1	27.4218	27.4218
P_4	0.0076	0.0076
P_6	0.0748	0.0748
P_8	0.0006	0.0006
P_{10}	399.4280	399.428
P_{12}	85.6184	85.6184
P_{15}	18.2351	18.2351
P_{18}	11.1616	11.1616
P_{19}	23.0465	23.0465

V_6	0.9940	1.0180
V_8	0.9940	1.0340
V_{10}	0.9940	1.0600

Table 14. Optimal settings of control variables of fuel cost minimization for different Technique on IEEE 118-bus system

Control Variable	Fmincon	TLBO [33]
V_{12}	0.9940	1.0133
V_{15}	0.9940	1.0063
V_{18}	0.9940	1.0033
V_{19}	0.9940	1.0039
V_{24}	0.9940	1.0221
V_{25}	0.9940	1.0385
V_{26}	0.9940	1.0600
V_{27}	0.9940	1.0106
V_{31}	0.9940	1.0019
V_{32}	0.9940	1.0077
V_{34}	0.9940	1.0121
V_{36}	0.9940	1.0105
V_{40}	0.9940	1.0014
V_{42}	0.9940	1.0036
V_{46}	0.9940	1.0219
V_{49}	0.9940	1.0347
V_{54}	0.9940	1.0075
V_{55}	0.9940	1.0067
V_{56}	0.9940	1.0070
V_{59}	0.9940	1.0205
V_{61}	0.9940	1.0192
V_{62}	0.9940	1.0190
V_{65}	0.9940	1.0591
V_{66}	0.9940	1.0461
V_{69}	0.9940	1.0600
V_{70}	0.9940	1.0325
V_{72}	0.9940	1.0218
V_{73}	0.9940	1.0288
V_{74}	0.9940	1.0256
V_{76}	0.9940	1.0255
V_{77}	0.9940	1.0446
V_{80}	0.9940	1.0570
V_{85}	0.9940	1.0546
V_{87}	0.9940	1.0523
V_{89}	0.9940	1.0600
V_{90}	0.9940	1.0400
V_{91}	0.9940	1.0429
V_{92}	0.9940	1.0523
V_{99}	0.9940	1.0435

V_{100}	0.9940	1.0476
V_{103}	0.9940	1.0371
V_{104}	0.9940	1.0261
V_{105}	0.9940	1.0229
V_{107}	0.9940	1.0166
V_{110}	0.9940	1.0185
V_{111}	0.9940	1.0255
V_{112}	0.9940	1.0101
V_{113}	0.9940	1.0149
V_{116}	0.9940	1.0522
T_8	0.9900	0.9904
T_{32}	0.9900	1.0971
T_{36}	0.9900	1.0188
T_{51}	0.9900	1.0091
T_{93}	0.9900	0.9992
T_{95}	0.9900	1.0549
T_{102}	0.9900	0.9000
T_{107}	0.9900	0.9526
T_{127}	0.9900	0.9847
Fuel Cost (\$/h)	129,682.647	129,682.844

D. Overall Discussion

Across all nine scenarios and three test systems, the fmincon solver and PSO consistently deliver competitive or superior results compared to DE, SCA, MJAYA, SSA, CBA, OGSA, GSA, TLBO, and IMFO. PSO demonstrates a clear advantage on AP loss minimization, particularly as system size increases, attributed to its ability to explore high-dimensional search spaces without gradient information [12]. Fmincon, while less effective on voltage deviation for larger systems, proves highly reliable for fuel cost minimization due to the smooth, well-conditioned nature of that objective function [26], [27]. These findings affirm that the combined use of fmincon and PSO provides a robust and practically applicable framework for solving RPD problems in large-scale power systems

IV. CONCLUSION

Based on the result of the research conducted, it can be conclude that:

1. Reactive Power Flow (RPF) optimization represents a highly nonlinear and complex combinatorial optimization problem due to the presence of numerous control variables and operational constraints. In this study, the performance of the Fmincon solver and Particle Swarm Optimization (PSO) technique was investigated for minimizing active power losses, total voltage deviation, and fuel cost while satisfying all equality and inequality constraints of the power system.
2. The effectiveness and robustness of the proposed approaches were evaluated using three standard benchmark systems, namely the IEEE 30-bus, IEEE 57-bus, and IEEE 118-bus test systems. Simulation results demonstrated that both the Fmincon solver and PSO

technique successfully achieved optimal operating conditions and provided significant improvements in system performance. In particular, the obtained solutions resulted in lower active power losses, reduced voltage deviations, and minimized generation costs compared with several existing optimization methods reported in the literature.

3. Furthermore, the comparative analysis revealed that the proposed optimization techniques exhibit strong convergence characteristics and high computational efficiency when applied to large-scale power systems. The results confirm that both methods are capable of effectively handling the nonlinear nature and operational constraints of the RPF problem. Overall, the study highlights the potential of Fmincon and PSO as reliable and efficient tools for reactive power dispatch optimization, contributing to enhanced power system security, stability, and economic operation.

ACKNOWLEDGMENT

The author would like to express sincere gratitude to Prof. Dr. Tri Wrahatnolo, M.Pd., M.T. and Ifqi Firmansyah, S.T., M.T., Ph.D. for their invaluable guidance, support, and constructive suggestions throughout the completion of this research. Their expertise and encouragement have greatly contributed to the successful accomplishment of this study..

REFERENCES

- [1] M. S. Durairaj, D. P. S. Kannan, and D. D. Devaraj, "Multi-Objective VAR Dispatch Using Particle Swarm Optimization," *Int. J. Emerg. Electr. Power Syst.*, vol. 4, no. 1, 2005, doi: 10.2202/1553-779x.1082.
- [2] A. A. A. El Ela, M. A. Abido, and S. R. Spea, "Differential evolution algorithm for optimal reactive power dispatch," *Electr. Power Syst. Res.*, vol. 81, no. 2, 2011, doi: 10.1016/j.epsr.2010.10.005.
- [3] B. Shaw, V. Mukherjee, and S. P. Ghoshal, "Solution of reactive power dispatch of power systems by an opposition-based gravitational search algorithm," *Int. J. Electr. Power Energy Syst.*, vol. 55, 2014, doi: 10.1016/j.ijepes.2013.08.010.
- [4] Y. Zeng and Y. Sun, "Application of hybrid MOPSO algorithm to optimal reactive power dispatch problem considering voltage stability," *J. Electr. Comput. Eng.*, vol. 2014, 2014, doi: 10.1155/2014/124136.
- [5] S. Durairaj, D. Devaraj, and P. S. Kannan, "Genetic algorithm applications to optimal reactive power dispatch with voltage stability enhancement," *J. Inst. Eng. Electr. Eng. Div.*, vol. 87, no. SEPT., 2006.
- [6] J. A. Muckstadt and R. C. Wilson, "An Application of Mixed-Integer Programming Duality to Scheduling Thermal Generating Systems," *IEEE Trans. Power Appar. Syst.*, vol. PAS-87, no. 12, 1968, doi: 10.1109/TPAS.1968.292156.
- [7] N. Kaur and I. Singh, "Economic Dispatch Scheduling using Classical and Newton Raphson Method," *Int. J. Eng. Manag. Res.*, no. 3, 2015.
- [8] J. Kim and K. K. Kim, "Dynamic programming for scalable just-in-time economic dispatch with non-convex constraints and anytime participation," *Int. J. Electr. Power Energy Syst.*, vol. 123, 2020, doi: 10.1016/j.ijepes.2020.106217.
- [9] J. Qin, Y. Wan, X. Yu, and Y. Kang, "A Newton Method-Based Distributed Algorithm for Multi-Area Economic Dispatch," *IEEE Trans. Power Syst.*, vol. 35, no. 2, 2020, doi: 10.1109/TPWRS.2019.2943344.
- [10] S. K. Giri, A. Mohan, and A. K. Sharma, "Economic load dispatch in power system by hybrid swarm intelligence," *Int. J. Recent Technol. Eng.*, vol. 8, no. 3, 2019, doi: 10.35940/ijrte.C4411.098319.
- [11] T. Ding, R. Bo, F. Li, and H. Sun, "A Bi-Level Branch and Bound Method for Economic Dispatch with Disjoint Prohibited Zones Considering Network Losses," *IEEE Trans. Power Syst.*, vol. 30, no. 6, 2015, doi: 10.1109/TPWRS.2014.2375322.
- [12] Z. Xin-gang, L. Ji, M. Jin, and Z. Ying, "An improved quantum particle swarm optimization algorithm for environmental economic dispatch," *Expert Syst. Appl.*, vol. 152, 2020, doi: 10.1016/j.eswa.2020.113370.
- [13] W. M. Lin, F. S. Cheng, and M. T. Tsay, "An improved tabu search for economic dispatch with multiple minima," *IEEE Trans. Power Syst.*, vol. 17, no. 1, 2002, doi: 10.1109/59.982200.
- [14] J. Zhou *et al.*, "A multi-objective multi-population ant colony optimization for economic emission dispatch considering power system security," *Appl. Math. Model.*, vol. 45, 2017, doi: 10.1016/j.apm.2017.01.001.
- [15] J. K. Pattanaik, M. Basu, and D. P. Dash, "Improved real coded genetic algorithm for dynamic economic dispatch," *J. Electr. Syst. Inf. Technol.*, vol. 5, no. 3, 2018, doi: 10.1016/j.jesit.2018.03.002.
- [16] H. Liu, X. Shen, Q. Guo, and H. Sun, "A data-driven approach towards fast economic dispatch in electricity-gas coupled systems based on artificial neural network," *Appl. Energy*, vol. 286, 2021, doi: 10.1016/j.apenergy.2021.116480.
- [17] C. Takeang and A. Aurasopon, "Multiple of Hybrid Lambda Iteration and Simulated Annealing Algorithm to Solve Economic Dispatch Problem with Ramp Rate Limit and Prohibited Operating Zones," *J. Electr. Eng. Technol.*, vol. 14, no. 1, 2019, doi: 10.1007/s42835-018-00001-z.
- [18] M. Basu, "Improved differential evolution for economic dispatch," *Int. J. Electr. Power Energy Syst.*, vol. 63, 2014, doi: 10.1016/j.ijepes.2014.07.003.
- [19] P. Lokender Reddy and G. Yesuratnam, "A modified bacterial foraging algorithm based optimal reactive power dispatch," *Indones. J. Electr. Eng. Comput. Sci.*, vol. 13, no. 1, 2019, doi: 10.11591/ijeecs.v13.i1.pp361-367.
- [20] D. C. Secui, "A new modified artificial bee colony algorithm for the economic dispatch problem," *Energy Convers. Manag.*, vol. 89, 2015, doi: 10.1016/j.enconman.2014.09.034.
- [21] S. Mirjalili, "SCA: A Sine Cosine Algorithm for solving optimization problems," *Knowledge-Based*

- Syst., vol. 96, pp. 120–133, 2016, doi: 10.1016/j.knosys.2015.12.022.
- [22] E. E. Elattar and S. K. ElSayed, “Modified JAYA algorithm for optimal power flow incorporating renewable energy sources considering the cost, emission, power loss and voltage profile improvement,” *Energy*, vol. 178, 2019, doi: 10.1016/j.energy.2019.04.159.
- [23] R. Venkata Rao, “Jaya: A simple and new optimization algorithm for solving constrained and unconstrained optimization problems,” *Int. J. Ind. Eng. Comput.*, vol. 7, no. 1, pp. 19–34, 2016, doi: 10.5267/j.ijiec.2015.8.004.
- [24] S. Mirjalili, A. H. Gandomi, S. Zahra, and S. Saremi, “Advances in Engineering Software Salp Swarm Algorithm : A bio-inspired optimizer for engineering design problems,” vol. 114, pp. 163–191, 2017, doi: 10.1016/j.advengsoft.2017.07.002.
- [25] A. H. Gandomi and X. Yang, “Chaotic bat algorithm,” *J. Comput. Sci.*, vol. 5, no. 2, pp. 224–232, 2014, doi: 10.1016/j.jocs.2013.10.002.
- [26] MathWorks, “Fmincon,” 2021. .
- [27] M. Novac, E. Vladu, O. Novac, and A. Grava, “Aspects regarding the optimization of the induction heating process using differential evolution,” *J. Electr. Electron. Eng.*, vol. 5, no. 1, pp. 145–150, 2012.
- [28] S. Duman, Y. Sönmez, U. Güvenç, and N. Yörükere, “Optimal reactive power dispatch using a gravitational search algorithm,” *IET Gener. Transm. Distrib.*, vol. 6, no. 6, 2012, doi: 10.1049/iet-gtd.2011.0681.
- [29] K. Y. Lee, Y. M. Park, and J. L. Ortiz, “A United Approach to Optimal Real and Reactive Power Dispatch,” *IEEE Power Eng. Rev.*, vol. PER-5, no. 5, 1985, doi: 10.1109/MPER.1985.5526580.
- [30] M. S. Saddique *et al.*, “Solution to optimal reactive power dispatch in transmission system using meta-heuristic techniques—Status and technological review,” *Electric Power Systems Research*, vol. 178, 2020, doi: 10.1016/j.epsr.2019.106031.
- [31] E. E. Elattar and S. K. ElSayed, “Probabilistic energy management with emission of renewable micro-grids including storage devices based on efficient salp swarm algorithm,” *Renew. Energy*, vol. 153, 2020, doi: 10.1016/j.renene.2020.01.144.
- [32] S. Mugemanyi, Z. Qu, F. X. Rugema, Y. Dong, C. Bananeza, and L. Wang, “Optimal Reactive Power Dispatch Using Chaotic Bat Algorithm,” *IEEE Access*, vol. 8, 2020, doi: 10.1109/ACCESS.2020.2982988.
- [33] H. R. E. H. Bouchekara, M. A. Abido, and M. Boucherma, “Optimal power flow using Teaching-Learning-Based Optimization technique,” *Electr. Power Syst. Res.*, vol. 114, 2014, doi: 10.1016/j.epsr.2014.03.032.
- [34] M. A. Taher, S. Kamel, F. Jurado, and M. Ebeed, “An improved moth-flame optimization algorithm for solving optimal power flow problem,” *Int. Trans. Electr. Energy Syst.*, vol. 29, no. 3, 2019, doi: 10.1002/etep.2743.
- [35] C. Dai, W. Chen, Y. Zhu, and X. Zhang, “Seeker optimization algorithm for optimal reactive power dispatch,” *IEEE Trans. Power Syst.*, vol. 24, no. 3, 2009, doi: 10.1109/TPWRS.2009.2021226.